

Deformation and Flow of a Two-Dimensional Foam Under Continuous Shear

G. Debrégeas, H. Tabuteau and J.-M. di Meglio*
*Institut Charles Sadron, CNRS UPR 022,
6, rue Boussingault, 67083 Strasbourg Cedex, France*

(Dated: October 28, 2018)

We investigate the flow properties of a two-dimensional aqueous foam submitted to a quasistatic shear in a Couette geometry. A strong localization of the flow (shear banding) at the edge of the moving wall is evidenced, characterized by an exponential decay of the average tangential velocity. Moreover, the analysis of the rapid velocity fluctuations reveals self-similar dynamical structures consisting of clusters of bubbles rolling as rigid bodies. To relate the instantaneous (elastic) and time-averaged (plastic) components of the strain, we develop a stochastic model where irreversible rearrangements are activated by local stress fluctuations originating from the rubbing of the wall. This model gives a complete description of our observations and is also consistent with data obtained on granular shear bands by other groups.

PACS numbers: 83.80.Fg, 82.70.-y, 05.40.-a

Cellular materials, such as foams, concentrated emulsions, slurries, or granular materials, exhibit rheological properties that cannot be understood within the scope of standard solid or liquid mechanics [1, 2, 3]. For such systems, thermal energies are orders of magnitude lower than the typical energy required to relax the structural arrangements of their components; under small forces, the material remains trapped in a metastable configuration and exhibits a solid-like behavior. When submitted to a large enough stress however, it can be driven through a sequence of new metastable configurations, giving rise to a macroscopic flow. But the resulting flow field may still differ a lot from what would be expected for a molecular liquid.

Dry sand slowly flowing down an hourglass provides a simple example of such abnormal flow behaviors: the flow splits into a plug-like central region and a strongly sheared thin layer at the wall - a few particles wide - where most of the dissipative process occurs [4]. This spontaneous localisation of the strain in narrow regions of the material (the so-called shear bands) can be observed in many other situations such as shear, surface, or convective flows for instance [5, 6, 7, 8]. Shear banding actually controls most of the practical situations one has to face in soil mechanics and industrial handling of grains, and is also relevant to pyroclastic flows in geology (for a review on granular matter see [9]). This question has recently received a lot of attention from physicists, both theoretically and experimentally [10, 11], but a clear picture has not emerged yet.

By contrast, the possibility of shear banding in foams has been mostly ignored in the literature, and numerical or theoretical studies usually assume shear flows in foams to be uniform [2, 12]. The assumption that shear banding

is unique to granular matter can be misleading because it suggests that some peculiar aspects of granular flows, such as solid friction, particle rotation or dilatancy, are required to derive a shear band model.

In this Letter, we report the formation of shear bands in aqueous foams. We believe that foams may shed light on the dynamics of granular systems by evidencing the minimal set of ingredients needed to get shear banding. To that extent, foams constitute a much simpler model than granular systems since the basic bubble/bubble interactions which control the mechanical properties of the material are well known: elastic (stored) energy is related to an increase of the total interfacial area when the bubbles are distorted whereas dissipated energy is associated with neighbors swapping events (T_1 processes) inducing flows in the liquid films and vertices (for a review on foams, see [13]).

In order to probe the microdynamics of the foam, one needs to track the trajectory of each bubble during shearing. Since 3-D foams are inherently diffusive to light, we used a 2-D model foam - a monolayer of bubbles - submitted to a continuous slow shear in a Couette geometry. The setup was composed of an inner shearing wheel and an outer ring (of respective radius $R_0 = 71$ mm and $R_1 = 122$ mm) confined between two transparent plates separated by a 2 mm gap. To produce the foam, the cell was first hold vertically and partially filled with a controlled volume of soap/water solution. Bubbles were formed by blowing nitrogen gas through two small injection holes at different flow rates until the resulting foam reached the top of the cell. Once set horizontally, the foam rapidly attained a uniform wetness characterized by its liquid fraction $0.01 < \phi < 0.3$ (Fig. 1). This foaming procedure was chosen because it produces bidisperse disordered foams and therefore eliminates crystallisation. The mean diameters within each of the two populations of bubbles were of the order of 2 and 2.7 mm, with a mean deviation of 0.2 mm. These bubbles were large enough compared to the gap height so that they would not over-

*Also at Université Louis Pasteur and Institut Universitaire de France

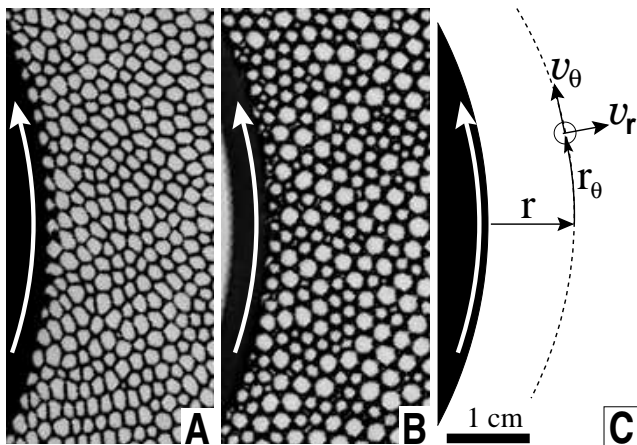


FIG. 1: Close-up frames of dry and wet 2-D foams under continuous shear. The shearing wheel appears in black. Notice the teeth shaped edge which eliminates slippage of the first row of bubbles. Arrows indicate the shearing direction. (A) A dry bidisperse foam ($\phi = 0.05$), showing deformed polygonal cells. (B) A wet bidisperse foam ($\phi = 0.20$). The bubbles are circular and undeformed. (C) System of coordinates used to analyze the flow field.

lap and form a truly two-dimensional foam. To define a bubble scale, we measured the mean distance d between first neighbors in the foam. In all experiments, d lay between 2.1 and 2.5 mm so that the gap between the wheel and the ring could accommodate from 20 to 25 rows of bubbles. The distance d was evaluated several times during the experiment and found to be almost constant. Coarsening would eventually lead to a growth of the biggest bubbles at the expense of the smallest ones, but over a longer time. We also checked the absence of shear induced size segregation that might have occurred during the experiment.

Shearing was induced by rotating the inner wheel at constant velocity V_{wheel} using a stepper motor. To avoid slippage at the wheel and the ring, their sides were teeth shaped so that the first and last rows of bubbles would remain irreversibly attached to the walls. To eliminate transient effects, we ran the experiment a full round before taking data. The motion of 1000 to 1500 bubbles was then recorded using a CCD digital camera positioned over the setup. In a typical experiment, 3000 images were taken corresponding to a total displacement of $600d$ of the wheel edge. The apparent centers of mass of the bubbles were subsequently tracked by image analysis (IDL software). To reduce the effect of the viscous friction between the bubbles and the confining plates, we restricted our study to quasistatic flows. We focused on average velocity measurements as a probe of shear rate dependence: we found that in the range $0 < V_{wheel} < 0.7 \text{ mm.s}^{-1}$, the velocity profiles were similar apart from an overall scale factor. All experiments were performed in the quasistatic regime at $V_{wheel} = 0.25 \text{ mm.s}^{-1}$. In the following, all velocities and distances are normalized by V_{wheel} and d

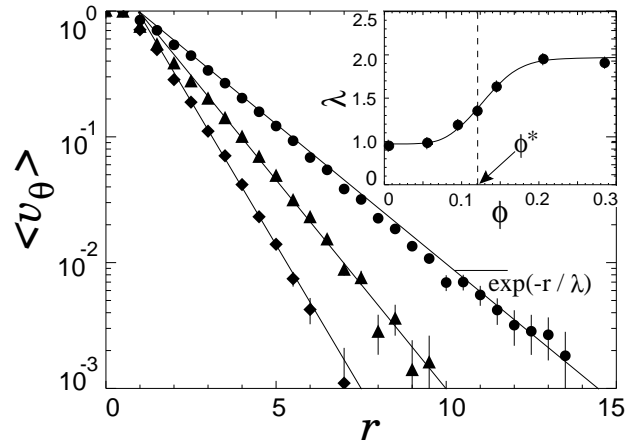


FIG. 2: Average tangential velocity profiles for different liquid fraction (\diamond : $\phi = 0.05$, \blacktriangle : $\phi = 0.12$, \bullet : $\phi = 0.20$), showing exponential decays with a width $\lambda(\phi)$. The small plateau for $0 < r < 1$ corresponds to the first row of bubbles being attached to the shearing wheel. Inset : dependence of λ on liquid fractions ϕ (the line is just a guide for the eyes). Two plateaus can be distinguished on either side of $\phi^* \simeq 0.12$, which separate deformed and undeformed bubbles regimes.

respectively. We note $\omega_0 = V_{wheel}/d$ the characteristic frequency of the shear.

Figure 2(A) shows the decay of the average tangential velocity $\langle v_\theta(r) \rangle$ with the distance r to the shearing wheel for different liquid fractions ϕ (see Figure 1(C) for variables definition). Averaging was performed over the tangential coordinate r_θ and time t , yielding smooth and reproducible profiles, although the instantaneous flow is strongly intermittent. The reduced velocity is found to approach 1 at $r \rightarrow 0$ confirming the absence of slip at the edge of the wheel. At larger r , the profiles exhibit an exponential decay :

$$\langle v_\theta(r) \rangle \sim \exp(-r/\lambda) \quad (1)$$

with a width λ depending on ϕ . The curve λ versus ϕ , presented on Figure 2(B), shows two plateaus at low and high volume fraction. The transition between these two regimes occurs around $\phi^* = 0.12$ which qualitatively marks the limit between dry foams with polygonal bubbles for $\phi < \phi^*$ and wet foams with undeformed bubbles for $\phi > \phi^*$. In both cases, the rapid decay of the mean velocity over a few bubble diameters, establishes the existence of shear banding in foams. The exponential shape of the velocity profile, observed in all experiments, appears as a robust feature which was also observed in comparable experiments performed on 2-D granular materials [4, 5, 14].

Beyond these time averaged profiles, the present setup allows measurements of the short timescale fluctuations of the bubbles velocities. A mere observation of the video sequences reveals brief oscillations of clusters of bubbles of various radial extension, rotating together as rigid bodies as shown in Figure 3. These dynamical structures

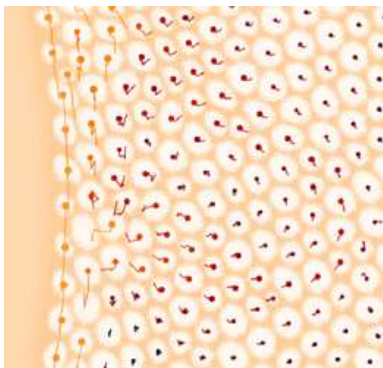


FIG. 3: Video frame of the foam with the position of the bubbles centers and their trajectories over the last 20 seconds. This time period corresponds to a total displacement of one bubble diameter for the first row (or equivalently for the inner disc edge). The dots size and lines color reflect the total distance travelled by the bubbles revealing a large rotating cluster.

are ephemeral and disappear after the wheel edge has moved by roughly one bubble diameter (this was checked by measuring time correlations of the velocity which we found decay to 0 in a time of the order of $1/\omega_0$). To quantitatively probe these coherent moves, we studied the spatial correlations of the instantaneous velocity field. We focused on the radial component v_r which has a zero time average and therefore gives a better signal to noise ratio (qualitatively, similar results were found when using $v_\theta - \langle v_\theta \rangle$ instead of v_r). Figure 4(A) shows the correlation function $g_r(\Delta r_\theta) = \langle v_r(r, r_\theta) \cdot v_r(r, r_\theta + \Delta r_\theta) \rangle / \langle v_r^2(r) \rangle$ for different values of r from 1 to 10, at a volume fraction $\phi = 0.20$. Regardless of r , g_r decreases with Δr_θ from 1 to a negative value then slowly relaxes to 0. The length $\xi(r)$ for which g_r reaches 0 defines a typical correlation length of the velocity field at a distance r . In Figure 4(B), r_θ has been rescaled by r . All the curves then collapse on a single one, which demonstrates a linear increase of $\xi(r)$ with the radial distance r : $\xi(r) = \alpha r$. Motivated by the observation of oscillating clusters, we modeled the flow field as a superimposition of rotating blocks of bubbles of various sizes (see figure caption for details) which allowed us to obtain a good fit of the master curve (Figure 4(B)). Similar results were obtained at all volume fractions, but the coefficient α was found to decrease with ϕ .

It is crucial to note that the velocity field which yields the measured correlation functions mainly corresponds to reversible movements of the bubbles centers, and thus probes the elastic deformation of the foam rather than the plastic flow. The quantity $\sqrt{\langle v_r^2 \rangle} / \langle v_\theta \rangle$ provides a good estimate of the ratio of reversible to irreversible moves of the bubbles occurring upon shearing. This quantity is larger than 1 beyond the first attached row of bubbles, and gets larger than 10 beyond the fifth row. The correlation measurements thus reveal that the instantaneous *stress* field is spatially correlated.

This peculiar characteristic of the foam deformation

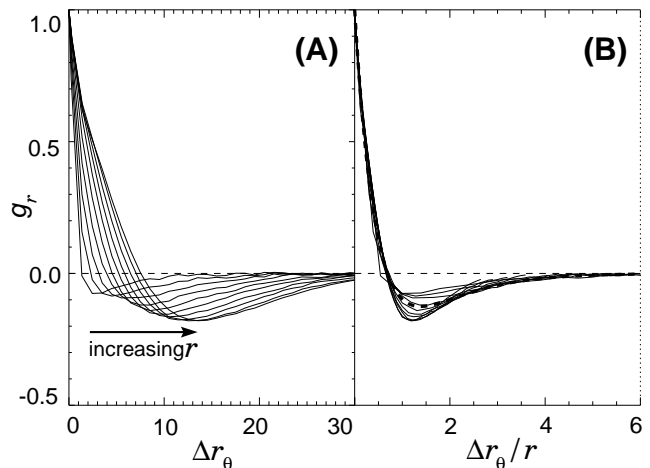


FIG. 4: (A): Spatial correlations of the radial velocity for different radial distances r from 1 to 10 ($\phi = 0.15$). (B): All correlations can be collapsed on a single curve when plotted versus the tangential distance rescaled by r . To fit this master curve, we assume that the radial velocity $v_r(r, r_\theta)$ at different r comes from the rotation of clusters of mean lateral extension $\xi(r)$ proportional to r ($\xi(r) = \alpha r$). The radial velocity field within a cluster of size μ is idealized by a two step function ($v_r = \epsilon v_0$ for $-\mu < r_\theta < 0$ and $v_r = -\epsilon v_0$ for $0 < r_\theta < \mu$ with $\epsilon = \pm 1$). We postulate a statistical distribution of μ around $\xi(r)$ by assuming that the fraction of clusters of size larger than μ is $\exp\left(-\frac{\mu}{\xi(r)}\right)$. The resulting correlation function (dotted line) then reads: $g_r(\Delta r_\theta) = \left(1 - \frac{\Delta r_\theta}{\alpha r}\right) \exp\left(-\frac{\Delta r_\theta}{\alpha r}\right)$.

field can actually be understood under the scope of linear elasticity, by simply modeling the foam as an isotropic elastic medium. During the initial loading, a uniform mean stress $\bar{\sigma}$ develops in the material (we neglect the radial geometry since the wheel radius is much larger than the shear band width). In the steady state, this uniform stress persists in average but is locally modulated by a fluctuating stress field $\Delta\sigma(t)$ of mean value 0 associated with the continuous rubbing of the wheel teeth. At each location ($r = 0, r_\theta = i$) on the wheel edge, the foam is indeed submitted to a localized perturbative stress $\Delta\sigma_i(t)$ of variance $s_0 = \langle \Delta\sigma_0^2 \rangle$ varying at a frequency ω_0 which elastically propagates into the material. These multiple noise sources add up to produce a stress fluctuation at a position (r, r_θ) of amplitude (see for instance [15]):

$$\Delta\sigma_r(r_\theta, t) \simeq \sum_i \frac{\Delta\sigma_i(t)}{\sqrt{r^2 + (r_\theta - i)^2}} \quad (2)$$

Assuming the noise sources to be uncorrelated ($\langle \Delta\sigma_i(t) \Delta\sigma_j(t) \rangle = 0$ for $i \neq j$), the resulting stress coherence length, at a distance r , takes the form $\xi(r) = \alpha r$, in agreement with our experimental findings. We interpret the different observed values for α as a signature of the anisotropy of the foam due to its initial loading. This is consistent with the observation of large values of α for

the driest foams where the largest uniform deformation is first produced. From Eq. 2, we are also able to compute the variance of the fluctuating stress $\Delta\sigma_r(t)$ as:

$$\langle \Delta\sigma_r^2 \rangle = s(r) \sim \frac{s_0}{\alpha r} \quad (3)$$

At this point, we wish to relate the fluctuating stress field $\Delta\sigma_r(t)$ to the measured average flow profile presented before, by taking into account the plastic property of the foam. Our approach mostly follows a model proposed by Pouliquen and Gutfraind [4] based on Eyring's activated process theory [16] to describe chute flows of granular materials. In the present description, the variance of the local stress fluctuation $s(r)$ plays the role of a temperature allowing plastic flow to occur. The moving boundary acts as a "hot wall", exciting internal deformation modes of the material in the form of self-similar rotating clusters. When the fluctuating stress overcomes a certain yield stress σ_y , the structure plastically yields. The yielding rate in the material by unit of time and space thus writes: $\omega = \omega_0 P(\sigma > \sigma_y)$ where $P(\sigma)$ is the density probability of stress. The stress at a distance r is a sum of $\sim r$ random variables (see Eq. 2) so that $P(\sigma(r))$ is a gaussian distribution centered on $\bar{\sigma}$ of variance $s(r)$. Using Eq. 3, the yielding rate at a distance r reads:

$$\omega(r) = \omega_0 P(\sigma(r) > \sigma_y) = \omega_0 \left(1 - \text{erf} \sqrt{\frac{r}{\lambda}} \right) \quad (4)$$

with

$$\lambda = \frac{1}{\alpha} \frac{2s_0}{(\sigma_y - \bar{\sigma})^2} \quad (5)$$

Each failure increments the average velocity gradient by 1 in reduced unit, so that the constitutive equation for the flow writes $\frac{\partial \langle v_\theta(r) \rangle}{\partial r} \sim -\omega(r)/\omega_0$ with the boundary conditions $\langle v_\theta(0) \rangle = 1$ and $\langle v_\theta(\infty) \rangle = 0$. A very good

approximate function to the integral of $\omega(r)$ is given by a pure exponential so that $\langle v_\theta(r) \rangle \simeq \exp(-r/\lambda)$.

This model gives the right form of the tangential velocity decay. An outcome of the model is contained in Eq. 5 which relates the α coefficient to the plastic flow decay length λ in the foam. Experimentally, we found $\alpha\lambda = 1.02 \pm 0.08$ (λ ranging from 1 to 2), which would suggest that $s_0/(\sigma_y - \bar{\sigma})^2$ is independent of the liquid fraction ϕ . This quantity is indeed self-adjusted via $\bar{\sigma}$ in the transient regime to allow enough rearrangements to occur.

In conclusion, we have observed shear banding in dry and wet 2-D foams under continuous slow shear and we have probed the associated elastic deformations of the foam, characterized by brief, collective oscillations of self-similar blocks of bubbles. We have developed a stochastic model which relates the plastic flow to the stress fluctuations experienced by the foam. The main characteristics of the flow (rapid decay of the average velocity over a few bubbles, large velocity fluctuations) are very similar to what is commonly observed in granular systems, suggesting that the proposed mechanism could remain valid for granular systems. As already mentioned, the predicted exponential velocity decay has been observed in various 2-D granular shear bands [4, 5, 7]. Moreover, the velocity profile in 3-D has been shown to obey a gaussian decay in the limit of disordered and non spherical grains [6]. This functional form for the velocity profile immediately follows from the modification of Eq. 3 in 3-D which then writes $s(r) \sim \frac{s_0}{\alpha^2 r^2}$ yielding a gaussian decay for $\langle v_\theta \rangle$.

Acknowledgments

We are grateful to D. Mueth for helping us with the image analysis. We wish to thank A. Kabla, S. Roux and C. Josserand for stimulating discussions.

-
- [1] P. Sollich, F. Lequeux, P. Hebraud, and M. Cates, *Phys. Rev. Lett.* **78**, 2020 (1997).
 - [2] S. A. Langer and A. J. Liu, *Europhys. Lett.* **49**, 68 (2000).
 - [3] A. Liu and S. Nagel, *Nature* **396**, 21 (1998).
 - [4] O. Pouliquen and R. Gutfraind, *Phys. Rev. E* **53**, 552 (1996).
 - [5] D. Howell, R. Behringer, and C. Veje, *Phys. Rev. Lett.* **82**, 5241 (1999).
 - [6] D. Mueth, G. Debrégeas, G. Karczmar, P. J. Eng, S. Nagel, and H. Jaeger, *Nature* **406**, 385 (2000).
 - [7] T. Komatsu, S. Inagaki, N. Nakagawa, and S. Nasuno, *Phys. Rev. Lett.* **86**, 1757 (2001).
 - [8] J. B. knight, E. E. Ehrichs, V. Kuperman, J. K. Flint, H. M. Jaeger, and S. R. Nagel, *Phys. Rev. E* **54**, 5726 (1996).
 - [9] P.-G. de Gennes, *Rev. Mod. Phys.* **71**, S374 (1999).
 - [10] J. Torok, S. Krishnamurthy, J. Kertesz, and S. Roux, *Phys. Rev. Lett.* **64**, 3851 (2000).
 - [11] G. Debrégeas and C. Josserand, *Europhys. Lett.* **52**, 137 (2000).
 - [12] D. J. Durian, *Phys. Rev. Lett.* **75**, 4780 (1995).
 - [13] D. Weaire and S. Hutzler, *The Physics of Foams* (Clarendon Press, Oxford, 1999).
 - [14] W. Losert, L. Bocquet, T. C. Lubensky, and J. P. Gollub, *Phys. Rev. Lett.* **85**, 1428 (2000).
 - [15] K. L. Johnson, *Contact Mechanics* (Cambridge University Press, 1985).
 - [16] K. Glasstone, J. Laidler, and H. Eyring, *The theory of rate processes* (McGraw-Hill, New-York, 1941).